

SOCIAL ISOLATION INDUCED BEHAVIOURAL AND MICROSTRUCTURAL DIFFERENCES IN JUVENILE MICE

Sarah Irwin
260806191

Integrated Program in Neuroscience
McGill University, Montreal
April 2020

A thesis submitted to McGill University in partial fulfillment of the
requirements of the degree of Master of Science.

© Sarah Irwin, 2020

Abstract

Myelin is a lipid-rich molecular bilayer that supports neuron function, stabilizes axons, helps synchronize neurotransmission, and remains plastic throughout life. The relationship between experience and adaptive myelination is best studied using animal models. Social isolation (SI) is a deprivation paradigm that elicits hypomyelination in the prefrontal cortex (PFC) and behaviour deficits including impaired sociability and increased anxiogenic behaviour. Implications of SI during the critical period of PFC development in mice was investigated with the goal of reproducing results of previous studies, exploring sex differences in vulnerability, and determining the ability of quantitative magnetic resonance imaging (MRI) to detect small differences in myelin *in vivo*.

60 (28 males) C57BL/6J mice were weaned at postnatal day 21, and housed in SI or as social controls for two weeks. Behaviour tests were conducted for sociability and anxiogenic behaviour, and in 48 mice (24 males) MRI scans were performed *in vivo* on a small bore 7 tesla scanner. Magnetization transfer ratio (MTR) and MT saturation (MTsat) maps were calculated using three FLASH images at 200 μ m isotropic resolution to estimate brain myelin content. MT-weighted images were used to detect local brain volume differences between groups using deformation based morphometry (DBM) analysis.

SI of male mice led to increased anxiogenic behaviour ($p=0.02$) compared to social controls. There was no difference in male or female sociability, or in female anxiogenic behaviour. DBM analysis did not reveal local anatomical differences between groups. The lack of variation in MTsat suggests there was little to no SI-induced hypomyelination in the PFC after two weeks of SI. MTR was increased in isolated males compared to controls in the limbic stress

circuit (hippocampus and amygdala). There was no significant relationship between anxiogenic behaviour and MTR results.

Postweaning SI produces a cascade of events that lead to altered synaptic plasticity and dendritic density in limbic areas. This likely accounts for the observed increase in male anxiogenic behaviour. Female mice are more resilient to SI, but preliminary data for an extended SI period of 4 weeks suggest that this may be a dose-dependent relationship. Previous studies show that a longer period of SI leads to a more pronounced myelin deficit and behavioural phenotype. A prolonged period of SI is required to evaluate the sensitivity of MRI to hypomyelination.

Résumé

La myéline est une membrane constituée d'une bicouche riche en lipides qui soutient la fonction neuronale, stabilise les axones, aide à synchroniser la neurotransmission et demeure plastique tout au long de la vie. La relation entre l'expérience et la plasticité de la myéline peut être étudiée en utilisant des modèles animaux. L'isolement social (SI) est un paradigme de privation qui provoque l'hypo-myélinisation du cortex préfrontal (PFC) et des déficits de comportement, y compris la sociabilité altérée et un comportement anxigène accru. Les implications de l'IS pendant la période critique du développement du PFC chez la souris ont été étudiées dans le but de reproduire les résultats d'études précédentes, d'explorer les différences de vulnérabilité entre les sexes, et de déterminer la capacité de l'imagerie par résonance magnétique (MRI) quantitative à détecter de petites différences de myéline *in vivo*.

60 souris (28 mâles) C57BL/6J ont été sevrées à 21 jours après la naissance, et logées en IS ou comme contrôles sociaux pendant deux semaines. Des tests de comportement ont été effectués pour la sociabilité et le comportement anxigène, et des scans MRI ont été réalisés *in vivo* chez 48 souris (24 mâles) sur un scanner 7 tesla. Des images quantitative du transfert de magnétisation (MTR et MTsat) ont été calculées en utilisant trois images FLASH à une résolution de 200 μ m isotrope pour estimer le contenu de la myéline du cerveau. Les images pondérées MT ont été utilisées pour examiner les différences locales de volume cérébral entre les groupes à l'aide d'une analyse par morphométrie basée sur les déformations (DBM).

Le SI des souris mâles entraîne une augmentation du comportement anxigène ($p = 0,02$) par rapport aux contrôles sociaux. Il n'y avait aucune différence dans la sociabilité mâle ou femelle, ou dans le comportement anxigène des femelles. L'analyse DBM n'a pas révélé de

différences anatomiques locales entre les groupes. L'absence de différence entre les groupes dans MTsat suggère qu'il y a peu ou pas d'hypo-myélinisation induite par le SI. La MTR a augmenté chez les mâles isolés par rapport aux contrôles dans le circuit de stress limbique (hippocampe et amygdale). Il n'y avait pas de relation significative entre le comportement et les résultats de la MTR.

Le SI après le sevrage produit une cascade d'événements qui conduisent à une altération de la plasticité synaptique et de la densité dendritique dans les zones limbiques. Cela explique probablement l'augmentation observée du comportement anxiogène des mâles. Les souris femelles sont plus résistantes à le SI, mais les données préliminaires pour une période SI de 4 semaines suggèrent que cela peut être une relation dose-dépendante. Des études antérieures montrent qu'une période plus longue de SI conduit à un déficit en myéline et à un phénotype comportemental plus prononcés. Une période prolongée de SI est nécessaire pour évaluer la sensibilité du MRI à l'hypo-myélinisation.

Table of Contents

Abstract	1
Résumé	3
List of Figures	6
List of Abbreviations	7
Acknowledgements	9
Contribution of Authors	9
1. Introduction	10
2. Literature Review	12
2.1 <i>Early Myelin Research</i>	12
2.2 <i>Role of Myelin in the CNS</i>	14
2.3 <i>Myelination During Development</i>	15
2.4 <i>Myelin Formation, Composition, and Mutation</i>	16
2.5 <i>Studying Myelin Plasticity</i>	18
2.6 <i>Social Isolation Paradigm</i>	19
2.6.1 <i>SI as a Model of Hypomyelination</i>	19
2.6.2 <i>SI-induced Disruption Throughout the Brain</i>	20
2.6.3 <i>“Isolation Syndrome”</i>	21
2.6.4 <i>Sexual Dichotomy</i>	22
2.7 <i>In vivo Myelin Mapping</i>	22
2.7.1 <i>Magnetization Transfer Imaging</i>	23
2.8 <i>Rationale and Objectives</i>	24
3. Methodology	25
3.1 <i>Social Isolation Paradigm</i>	26
3.2 <i>Behavioural Tests</i>	26
3.2.1 <i>Crawley’s Sociability Test</i>	27
3.2.2 <i>Elevated-Zero Maze</i>	28
3.3 <i>Magnetic Resonance Imaging</i>	28
3.4 <i>Tissue Fixation</i>	30
3.5 <i>Immunofluorescence</i>	30
3.6 <i>Data Analysis</i>	31
3.6.1 <i>Image Processing</i>	31
3.6.2 <i>Statistical Analysis</i>	32
4. Results	33
4.1 <i>Crawley’s Sociability Test: No effect</i>	33

4.2 Elevated-Zero Maze: Increased anxiogenic behaviour in males	34
4.3 Imaging-based brain morphometry and microstructure	35
5. Discussion	35
5.1 No Difference in Sociability	36
5.2 Elevated Anxiogenic Behaviour in Isolated Males	37
5.3 Increased MTR in Limbic System	38
5.4 Limitations	39
6. Conclusion	41
References	42

List of Figures

Figure 1: Historic images demonstrating the progression of myelin research	13
Figure 2: Behaviour test apparatus	27
Figure 3: MT-weighted image of one mouse brain acquired using FLASH sequence	29
Figure 4: Sample images representing data to be acquired for histological validation of MRI results	31
Figure 5: Sociability test results	33
Figure 6: Anxiogenic behaviour test results	34
Figure 7: MTR results	35

List of Abbreviations

AMG	Amygdala
ASD	Autism Spectrum Disorder
BDNF	Brain-derived neurotrophic factor
CNS	Central nervous system
CoBra	Computational Brain Anatomy
DBM	Deformation-based morphometry
DNA	Deoxyribonucleic acid
DWI	Diffusion weighted imaging
EPI-DA	Echo planar imaging double-angle
FLASH	Fast low angle shot
GABA	Gamma-Aminobutyric acid
Hipp	Hippocampus
HPA	Hypothalamic-pituitary-adrenal
Iba-1	Ionizing calcium-binding adaptor molecule 1
IF	Immunofluorescence
MAG	Myelin-associated glycoprotein
MBM	MICe-build-model
MBP	Myelin basic protein
MRI	Magnetic resonance imaging
MT	Magnetization transfer

MTR	Magnetization transfer ratio
MTsat	Magnetization transfer saturation
NAcc	Nucleus accumbens
NL3	Neuregulin III
OCT	Optimal cutting temperature
ODC	Oligodendrocyte
OPC	Oligodendrocyte progenitor cell
PBS	Phosphate buffered saline
PD	Proton density
PFA	Paraformaldehyde
PFC	Prefrontal cortex
PLP	Proteolipid protein
PMD	Pelizaeus-Merzbacher disease
PN	Post-natal day
PNS	Peripheral nervous system
RF	Radio frequency
ROI	Region of interest
SI	Social isolation
SZ	Schizophrenia
VFA	Variable flip angle
WM	White matter

Acknowledgements

I would like to thank my supervisor Christine Tardif for the many opportunities she has afforded me, and for her diligent support and encouragement. I would like to recognize the industrious efforts and care taken by Marius Tuznik, the MRI technician for the Small Animal MRI Unit. I extend my gratitude to my advisory committee David Rudko and Mallar Chakravarty, the members of the Tardif Lab, and the staff at the MNI's Center of Neurological Disease Models for their generous guidance. Thank you to Daryan Chitsaz (Kennedy Lab) and Sabrina Quilez (Cloutier Lab), who were instrumental in tissue preparation, protocol development, and data collection for immunofluorescence. Thank you to Gabriel Devenyi who guided MRI image processing and analysis, to Thomas Stroh who shared his lab space and materials, and to Behrang Sharif for providing the MRI mouse bed. Finally, thank you to my family for their immense love and faith in me, and to all the lab animals whose lives are sacrificed for science.

Contribution of Authors

This thesis is the original and independent work of Sarah Irwin, supervised by Dr. Christine Tardif. Behavioural data collection and analyses were performed by the author. Magnetic resonance imaging was performed by the author and Marius Tuznik with the help of Dr. David Rudko. MRI image processing and analysis was performed by Dr. Christine Tardif with the help of Dr. Gabriel Devenyi and Dr. Mallar Chakravarty. Immunofluorescence protocol development and data collection was performed by Daryan Chitsaz. All experiments were performed in accordance with the Canadian Council on Animal Care and approved by the McGill University Animal Care Committee, under Animal Use Protocol 2018-7993.

1. Introduction

Myelin is a molecular bilayer composed of proteins and lipids, which stabilizes axons, facilitates neural communication via saltatory conduction, and supports neuron function and metabolism. It aids in the formation of stable networks during development, and remains plastic throughout the lifetime to adapt to an organism's environment (Kandel, Schwartz, Jessell, Siegelbaum, & Hudspeth, 2013). The relationship between experience and adaptive myelination can be exploited to better understand the dynamics of myelination across a lifetime (Kaller, Lazari, Blanco-Duque, Sampaio-Baptista, & Johansen-Berg, 2017).

Myelination impacts all brains, whether healthy or unhealthy. Hypomyelination has been reported in psychiatric disorders such as schizophrenia (SZ), Autism Spectrum Disorders (ASD), anxiety, and depression (Regenold et al., 2007). The underlying mechanisms of these disorders are not well understood, an issue that can lead to trial-and-error based treatment strategies. It is imperative that we continue to build on the foundation of myelin research with the hope of shedding light on the molecular mechanisms behind these disorders. To do so, animal models are needed to first establish causality in the relationship between myelination and experience in the brain.

Social isolation (SI) is a form of deprivation paradigm used in mice to elicit hypomyelination in the prefrontal cortex (PFC). Recent studies have identified a critical period in the development of the mouse brain during which myelination of the PFC is sensitive to SI (Makinodan, Rosen, Ito, & Corfas, 2012). This hypomyelination is accompanied by a behavioural phenotype including altered sociability (Matthews et al., 2016; Okada et al., 2015; Pais et al., 2019), and increased anxiogenic behaviour (Lander, Linder-Shacham, & Gaisler-Salomon, 2017;

Makinodan et al., 2012). Deficits in these PFC-dependent behaviours are comparable to the behavioural phenotypes seen in patients suffering from the psychiatric disorders listed above, and share a similar sexual dichotomy (Bangasser & Valentino, 2014). While research on SI in female rodents is limited, female mice tend to be more resilient to paradigms similar to SI than their male counterparts (Fone & Porkess, 2008; Hinton, Li, Allen, & Gourley, 2019; Pietropaolo, Singer, Feldon, & Yee, 2008).

Myelin quantification requires a non-invasive imaging tool for use *in vivo*. Magnetic resonance imaging (MRI) offers the opportunity to acquire data at multiple timepoints, allowing for the longitudinal investigation of adaptive myelination. Magnetization transfer (MT) imaging can be used as an indirect measure of myelin content, and has been validated in rodent models of myelination (Helms, Dathe, Kallenberg, & Dechent, 2008; Poggi et al., 2016). The development of an imaging protocol for a whole-brain high-resolution MT saturation map will provide a unique tool for use in longitudinal studies and conditional knockout models of myelination.

This project aims to address the lack of causality in the relationship between adaptive myelination and experience, while taking sex differences into account. A two-week SI paradigm is used to induce hypomyelination in the PFC of young adolescent mice. An MT imaging protocol sensitive enough to study myelination in mice *in vivo* is optimized and validated. This data, in combination with behaviour tests for sociability and anxiogenic behaviour, provide further evidence in support of the relationship between experience, myelination, and behaviour relative to sex in mice.

2. Literature Review

2.1 Early Myelin Research

The term myelin was coined during the mid-19th century by Rudolf Virchow, the “father of pathology” (Kettenmann & Ransom, 2013). The visual distinction between white and grey matter was first made by the anatomist Vesalius (Figure 1a) three hundred years earlier (Vesalius, 1543). Using magnifying lenses, scientists struggled to determine the structure and function of the mysterious “nerve marrow” surrounding “brain tubes.” The 1830’s brought the microscope revolution in Germany, allowing scientists to delve deeper (Lister, 1830). In 1839, Theodor Schwann published observations describing the neurilemma of Schwann cells in the peripheral nervous system (PNS), and the lack thereof on the myelin of the central nervous system (CNS) (Schwann, 1911).

This investigation hit a dead end until the advent of the osmium stain (Schultze & Rudneff, 1865), a technique put to use by Ranvier in the 1870’s. In collaboration and competition, researchers sought to clarify the structure and development of the myelin sheath. Shortly before the First World War, Santiago Ramón y Cajal’s masterful use of precious metal impregnation staining sparked the false theory that myelin is secreted from the axon (Cajal, 1912). Cajal’s pupil, Pío del Río-Hortega developed the silver carbonate staining method, through which he discovered oligodendroglia processes wrapping around myelin (Figure 1b), a finding that contradicted his mentor’s theory of axonal secretion (del Río-Hortega, 1921). He enlisted the help of Wilder Penfield, who later went on to found the Montreal Neurological Institute. Together, they endeavored to substantiate the role of oligodendrocytes (ODCs) in the formation and support of myelin (Penfield, 1924).

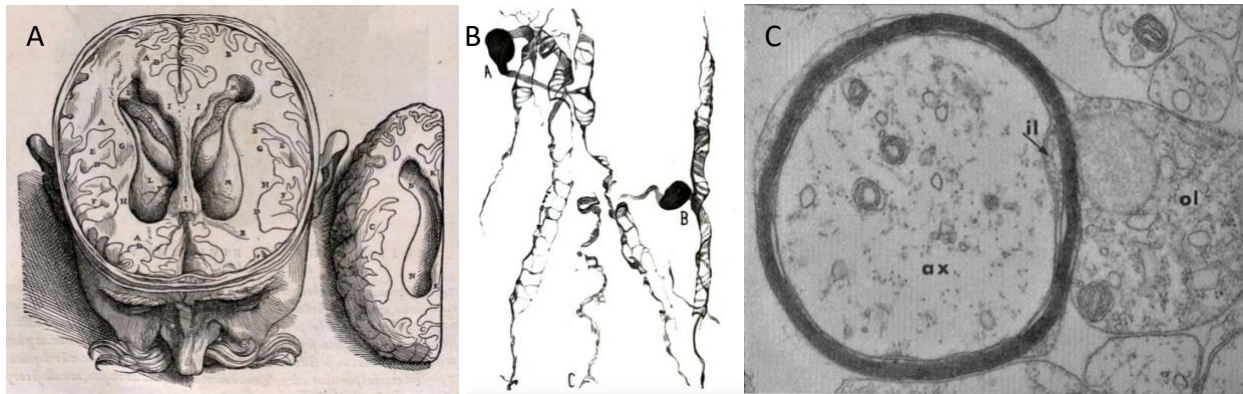


Figure 1: Historic images demonstrating the progression of myelin research

- a) Plate 608 from De Humani Corporis Fabrica showing a coronal section with distinction between grey and white matter (Vesalius, 1543)*
- b) Illustration of a silver carbonate stain showing ODC processes coiled around myelin (Fig. 58, Hortega, 1928)*
- c) Electron micrograph showing the plasma membrane of an ODC process forming a myelin sheath around and axon (Fig. 7, R. P. Bunge, 1968)*

As novel techniques were developed and refined, they were used by researchers attempting to theorize myelin’s membrane architecture. Tools including light microscopy, X-ray diffraction, and electron microscopy eventually served to reveal myelin’s spiraled layers and g-ratio (axon diameter/fiber diameter) tendencies. The advancement of fixation techniques allowed for the improved use of electron microscopy in the CNS (Boullerne, 2016). In 1962, Richard and Mary Bunge were able to demonstrate that CNS myelin is produced by ODCs (Figure 1c), and that these glial cells could myelinate multiple internodes on more than one axon (M. B. Bunge, Bunge, & Pappas, 1962). A decade later, William Norton developed a method for the purification of CNS myelin, finally allowing for the in-depth study of its biochemical composition (Norton & Poduslo, 1973).

Throughout the history of myelin research, the advancement of knowledge has been limited by the tools and techniques available. New techniques are required to capture the

dynamic nature of myelin, a process that remains poorly understood, yet is largely implicated in the functioning of both healthy and unhealthy nervous systems across the lifespan.

2.2 Role of Myelin in the CNS

Neurons are the basic information processing units in the nervous system. Simply put, their role is to receive input, process the information, and release output onto receiving cells. Neuronal function is supported in many ways by glial cells like ODCs. From providing structural stability and nutrients to waste removal, glial cells play a critical role in maintaining the homeostasis of each neuron (Fields et al., 2014). On a grand-scale, this allows networks in the nervous system to function in equilibrium, transmitting signals effectively and efficiently.

Neurons communicate by transmitting electrical signals, called action potentials, from the initiation segment in the cell body, along the axon, to the terminal button. From here, the information is passed on to the next neuron through dendritic synapses as an electrical or chemical signal. The action potential may be propagated over lengths of 0.1 mm to 2 m, depending on the type of neuron. This signal has a constant amplitude of 100 mV, and speeds ranging from 1 to 100 m/s (Kandel et al., 2013). This constancy is maintained by periodic regeneration of the signal as it moves along the axon. Action potential propagation is facilitated by myelin, a lipid-rich bilayer produced by ODC processes that coil around the axon (Figure 1c). The myelinated regions, called internodes, are separated by nodes of Ranvier. The nodes are unmyelinated gaps on the axon where action potential regeneration takes place. Voltage-gated ion channels are concentrated in these nodes to allow for extracellular ion exchange. Myelinated neurons are able to conduct action potentials more rapidly and efficiently because myelin acts as an electrical insulator for the axon, and the signal “jumps” between nodes. The

depolarizing action potential is triggered in the cell body, but would die out before reaching the terminal button without saltatory conduction. At each unmyelinated node, the decreasing amplitude of the action potential is replenished and propagated by a rapid influx of sodium ions. This allows the signal to continue its journey along the axon. Conversely, in unmyelinated neurons, the action potential is slowed, or even blocked from transmission (Kandel et al., 2013; Purves et al., 2001).

The amount of myelination varies between neurons to produce precisely synchronized conduction times on the larger scale (Fields, 2015). This adaptation aids in all nervous system communication, from producing appropriate responses to sensory stimuli, to the maintenance of intrinsic oscillatory rhythms (Pajevic, Basser, & Fields, 2014). The ability to customize the speed of signal transmission is crucial to the proper functioning of both central and peripheral nervous systems.

2.3 Myelination During Development

In normal human development, the brain grows and stabilizes, progressing through a series of critical periods. At the end of each of these expansive stages, neuronal arborization stops, and myelin forms to stabilize favourable synaptic arrangements. If the myelin fails to develop at this time, growth and maturation can continue past the end of the normal critical period (Kandel et al., 2013). In the CNS, myelination begins in the visual system one to two months before birth, and continues through other sensory systems to reach the PFC within the first year of life. These myelinated regions continue to mature into the third decade, and they remain plastic even longer (Levitt, 2003; Paus et al., 2001). Once the brain stops developing, myelin degrades with age, leading to decreased white matter integrity. This myelin loss impairs

synaptic functioning, and is most prominent in the prefrontal and temporal cortices. Myelin loss in these regions is related to the cognitive deficits that accompany old age (Chapman & Hill, 2020; Kandel et al., 2013).

During gestation, oligodendrocyte progenitor cells (OPCs) migrate from the neuraxis to proliferate throughout the CNS. OPC proliferation and subsequent myelination are regulated by signaling between axons, OPCs, and ODCs, and are dependent on neuronal activity. Neuregulin III (NL3), a secreted protein, and Brain Derived Neurotropic Factor (BDNF) moderate OPC proliferation. Receptors at axon-OPC contacts allow glutamate and gamma-Aminobutyric acid (GABA) signaling to regulate the transition from proliferation to ODC differentiation.

Differentiated ODCs are able to myelinate axons with little guidance, however the receptors on these cells are responsive to neuronal activity through glutamate and calcium release onto ODCs (Baraban, Mensch, & Lyons, 2016). Mice that are unable to generate newly differentiated ODC's show learning deficits (Richardson et al., 2014), indicating that presence of ODCs and their communication with neurons allow for plasticity to continue through adulthood.

2.4 Myelin Formation, Composition, and Mutation

In the CNS, tissue can be distinguished as grey matter (GM) and white matter (WM), where GM consists of more neuronal cell bodies and fewer myelinated axons than WM. Three to four percent of the cell population of GM, and eight to nine percent of WM is made of OPCs, which differentiate into mature ODCs (Dawson, Polito, Levine, & Reynolds, 2003; Tomlinson, Leiton, & Colognato, 2016). As described above, the processes of these glial cells form the myelin sheath. Each ODC can myelinate up to thirty axons by projecting extensions of its plasma membrane to coil around nearby neurons (Figure 1c). Once contact has been made between

the ODC extension and the axon, the ODC process coils around the neural fiber until the two extracellular surfaces adhere to each other. As the ODC continues to wrap around the neuron, compaction takes place, and membrane-bound proteins are synthesized and integrated into the sheath. This tightening of the layers leads to a spiral array of membrane alternating with aqueous extracellular and cytoplasmic compartments (Deber & Reynolds, 1991; Quarles, Macklin, & Morell, 2006). This process is driven and regulated by signaling between the glial cells and the axon. After development, this two-way signaling maintains the health of the ODCs and the neuron, as well as the integrity of the myelin (Baraban et al., 2016; Nave & Trapp, 2008; Taveggia, Feltri, & Wrabetz, 2010).

The dry matter of the myelin sheath is composed of bimolecular layers of lipids (70%) and proteins (30%). The lipid portion is primarily made of cholesterol and phospholipid. The two most abundant proteins in the myelin sheath are proteolipid protein (PLP) and myelin basic protein (MBP). While MBP sits on the cytoplasmic surface of myelin, PLP lies integrally. These two proteins may play a role in initiating the process of compaction, maintaining the structural stability of the myelin sheath, and have therefore been implicated in myelination and demyelination (Deber & Reynolds, 1991; Kandel et al., 2013; Quarles et al., 2006). Myelin-associated glycoprotein (MAG) is another important cell-surface protein thought to play a role in cell-to-cell recognition and interactions (Deber & Reynolds, 1991).

Because myelin formation and structural maintenance depend on adequate functioning of myelin-integrated proteins, mutations in the genes that code for them can be disastrous for neuronal function. Such mutations result in a variety of demyelinating diseases in humans, some of which have been studied using animal models. For example, the *jimpy* mouse is a PLP

knockout model that causes abnormal layering of myelin and ODC apoptosis (Quarles et al., 2006). This model is comparable to the human disease Pelizaeus-Merzbacher disease (PMD), a disorder caused by severe hypomyelination. Since the PLP gene is on the X-Chromosome, PMD is hereditary and occurs primarily in males (Hudson, 2003; Scherer, 1997). The *jimpy* mouse and other animal models of demyelination have been used to better understand the role that myelin-integrated proteins play in myelin formation, function, and maintenance.

2.5 Studying Myelin Plasticity

Myelination remains dynamic past development, often changing in response to environmental experience. Myelin remodeling occurs along single axons, influencing conduction times. Old sheaths are replaced with new ones, large gaps are filled, and unmyelinated axons are myelinated. Conversely, myelin can also shrink adaptively to synchronize communication within the CNS. The potential for myelin regeneration varies between brain regions, neuron types, and circuitry (Baraban et al., 2016).

Human neuroimaging studies have revealed changes in white matter quantities as a result of physical activities such as practicing the piano and aerobic fitness (Bengtsson et al., 2005; Scholz, Klein, Behrens, & Johansen-Berg, 2009; Voss et al., 2013). To investigate the relationship between experience, biology, and behaviour more intimately, researchers commonly use rodent models of experience-induced adaptation. Enrichment-based paradigms such as voluntary exercise and environmental enrichment lead to enhanced ODC lineage and myelination. Deprivation-based paradigms have the opposite effect (Tomlinson et al., 2016; Zhao et al., 2012). Whether enrichment- or deprivation-based, the outcomes of these paradigms are affected by critical periods of development (De Villers-Sidani, Chang, Bao, &

Merzenich, 2007). Experiential paradigms are generally more effective in young animals than in adults because the brain's plasticity decreases with age.

2.6 Social Isolation Paradigm

Social isolation (SI) is a form of deprivation paradigm used to model more than just loneliness. Makinodan *et al.* (2012) identified a critical period between post-natal days (PN) 21 and 35, during which PFC myelination is sensitive to SI. Compared to controls, isolated mice exhibit behavioural deficits along with long-lasting changes in ODCs and heterochromatin, as well as thinner myelin sheaths (Liu *et al.*, 2012; Makinodan *et al.*, 2012). These findings correspond with studies of SI and loneliness in humans. Children who experience isolation and neglect show impaired cognition, impulsivity, attention and social deficits, and decreased PFC activation (Chugani *et al.*, 2001).

2.6.1 SI as a Model of Hypomyelination

SI-related hypomyelination poses a unique opportunity of study. SI in juvenile and adult mice leads to abnormal ODC morphology with fewer branches, decreased myelin thickness, myelin gene transcripts (MBP, MAG), and NG3 transcripts in the PFC (Makinodan *et al.*, 2012). In prolonged isolation (8 weeks), decreased nuclear chromatin compaction and increased histone acetylation in the PFC provide evidence for isolation-induced epigenetic changes related to immature ODCs and hypomyelination (Liu *et al.*, 2012). In juvenile mice isolated for just two weeks from post-natal (PN) day 21 to 35, biological and behavioural effects are not reversed by reintegration with social mice. Conversely, mice isolated for 4 weeks starting after this critical period (PN 35-65) regained normal biological and behavioural phenotypes (Makinodan *et al.*, 2017, 2012).

The period from PN 21 to 35 is equated to early to mid-adolescence in mice. This is an age of acute vulnerability to adversity, specifically social stress in both humans and animal models. During this time, PFC neurons undergo drastic structural reorganization and synaptic remodeling (Agoglia et al., 2017). Dendritic spines and synapses are stabilized and refined. In some regions, up to 50% of these connections are pruned (Palanza, 2001). This reorganization depends heavily on the experience of the animal during this time, especially through social play and environmental stimuli (Bell, Pellis, & Kolb, 2010). It follows that the deprivation of this necessary social-sensory input would put normal development at risk.

2.6.2 SI-induced Disruption Throughout the Brain

In addition to deficits in myelination, SI has been linked to alterations in excitatory, inhibitory and catecholaminergic signalling, and stress-circuitry hyperactivation making socially isolated rodents a strong model for human psychiatric disorders.

Juvenile SI in particular has been used as a model of early-life chronic stress in rodents. Such stressors cause a variety of persisting changes in cellular and molecular structure and function in the CNS. SI induces hyperactivity of the hypothalamic-pituitary-adrenal (HPA) stress axis, which instigates a cascade of damaging molecular changes in the cortex. This includes oxidative and nitrosative stress that cause mitochondrial dysfunction and results in cellular energy deficiency (Chen, Spiers, Sernia, & Lavidis, 2015; Haj-Mirzaian et al., 2016; Maes, Galecki, Chang, & Berk, 2011).

Many SI-induced modifications in morphology and signalling have been studied in the cortico-limbic regions of the brain. Cortisol toxicity has been linked to decreased dendritic spine density and altered glutamate synapse functionality in the medial PFC (Amiri et al., 2016;

Matsumoto, Fujiwara, Araki, & Yabe, 2019). Increased glutamate signalling in the PFC and hippocampus (Hipp) leads to excitotoxicity explained by upregulation of glutamate receptors in these regions. This disrupts the regulation of dopamine and serotonin signalling in the PFC and nucleus accumbens (NAcc) (Kawasaki et al., 2011; Toua, Brand, Möller, Emsley, & Harvey, 2010; Yamamuro et al., 2018). In addition, dendritic atrophy and increased expression of some GABA receptor subunits in the Hipp and dentate gyrus affect synaptic transmission of GABA (Haj-Mirzaian et al., 2016; Matsumoto, Puia, Dong, & Pinna, 2007).

These alterations in circuitry and signalling are reminiscent of the core neural correlates of depression, anxiety, and schizophrenia (Andersen & Teicher, 2008; Matsumoto et al., 2019). The various components involved in widespread SI-induced disruption in the brain have not yet been directly linked to hypomyelination, however it is likely that these mechanisms influence one another. Since the progression of myelination *in vivo* can be followed non-invasively and longitudinally, its study is a step towards understanding how myelin adaptation may relate to coinciding neural changes.

2.6.3 “Isolation Syndrome”

The behavioural components of “isolation syndrome” were first described in the 1970’s (Valzelli, 1973), and have been thoroughly expanded on since. SI has been linked to anxiety- and depressive-like behaviours, increases in aggression, reduced prepulse inhibition, altered sociability, learning, and even mobility in some strains (Amiri et al., 2016; Chang, Hsiao, Chen, Yu, & Gean, 2015; Lim, Taylor, & Malone, 2011; Medendorp et al., 2018; Wongwitdecha & Marsden, 1996). Altered sociability (Matthews et al., 2016; Okada et al., 2015; Pais et al., 2019) and increased anxiety-like behaviour (Lander et al., 2017; Makinodan et al., 2012), have been

shown to correspond with hypomyelination of the PFC, whether induced by SI or genetic model (Haj-Mirzaian et al., 2016; Murínová, Hlaváčová, Chmelová, & Riečanský, 2017; Poggi et al., 2016).

2.6.4 Sexual Dichotomy

It is important to recognize that the majority of previous research has been conducted using only male animals. The extent to which sex influences vulnerability to SI remains unclear. Some studies suggest that oestrogen may provide a neuroprotective mechanism, making females more resilient to social stress (Ferdman, Murmu, Bock, Braun, & Leshem, 2007; Palanza, 2001; Palanza, Gioiosa, & Parmigiani, 2001). In the few studies that have observed SI in females, differences between sexes were recorded in both biology and behaviour in response to SI (Chadda & Devaud, 2004; Hinton et al., 2019; Pietropaolo et al., 2008). This dichotomy is representative of the sex differences observed in human psychiatric illness (Qiu et al., 2018). For example, in schizophrenic patients, average age of onset is earlier, and symptoms are more severe in men than in women (Pietropaolo et al., 2008).

2.7 *In vivo* Myelin Mapping

In vivo myelin imaging is needed to capture the complexity of the dynamic nature of adaptive myelination. Longitudinal data collection is needed to study the impact of deprivation paradigms on myelin plasticity across the lifespan, and how this trajectory differs between individuals. *Ex vivo* quantification techniques are myelin-specific, but do not allow for longitudinal manipulation within subjects. There are a variety of methods to turn to when choosing to study myelination *in vivo*.

The visualization of living cells in transparent animal models like the transgenic zebrafish or xenopus tadpole is powerful when used to study genetic expression and CNS development in real-time (Bin & Lyons, 2016). However, these models do not lend themselves to the study of experience-induced myelination and behaviour to the same extent as rodent models do. Optical imaging techniques such as bioluminescence and fluorescence imaging can be used to acquire high resolution quantitative data in rodents, however they can be invasive and are not powerful enough to image subcortical structures without a cranial window (Aswendt, Adamczak, & Tennstaedt, 2014). Both transparent animal models and optical imaging techniques are preclinical modalities, limiting the translational impact of the research.

On the other hand, MRI, a clinical tool, can be performed in humans and animal models. (Wang et al., 2011). The ability of MRI to capture high resolution whole-brain images at multiple timepoints both in rodents and humans sets it apart from other *in vivo* imaging techniques.

2.7.1 Magnetization Transfer Imaging

MRI is a non-invasive technique that uses a strong static magnetic field, spatial magnetic field gradients, and radio frequency (RF) pulses to gain information about anatomy and physiological processes in the body. RF pulses excite the nuclear spins of hydrogen protons in the tissue. As the spins relax and decay back to equilibrium, spatial gradients are applied to encode the spins' position and a signal is measured using a RF coil. Changing the pulse sequence parameters allows for the images to be acquired with various contrasts depending, for instance, on the relaxation times of different tissue types (McRobbie, Moore, Graves, & Prince, 2006).

In humans, white matter imaging has mainly relied on diffusion weighted imaging (DWI) to quantify changes in myelin. However, because this technique depends on the motion of water molecules in nerve fibers, it is influenced by other microstructural factors (Heath, Hurley, Johansen-Berg, & Sampaio-Baptista, 2018). Magnetization transfer (MT) imaging can be used as a more specific indirect measure of myelin content. In MT imaging, an RF pulse is applied to saturate water protons bound to myelin macromolecules, but not the free water. Energy is exchanged between the bound and free pools (Heath et al., 2018), such that the magnetization of the observable free water pool is decreased. In MT ratio (MTR) imaging, an image with a MT saturation pulse is normalized by an image acquired with identical scan parameters but without a MT pulse (Fralix, Ceckler, Wolff, Simon, & Balaban, 1991). The acquisition of a third T1-weighted image allows to remove bias from the T1 relaxation time and RF field non-uniformity, resulting in a more specific estimate of the MT saturation (MTsat). These techniques have been effective in rodent models of demyelination and remyelination, and has been validated with histology (Helms et al., 2008; Poggi et al., 2016).

2.8 Rationale and Objectives

This project builds on the findings that social isolation induces behavioural deficiencies, and biological changes in ODCs and myelin in the PFC (Liu et al., 2012), and that the critical period of behavioral and biological sensitivity to social isolation in young mice is from postnatal day 21 to 35 (Makinodan et al., 2012). The objective of this study is (1) to optimize and validate a multi-modal quantitative MRI protocol sensitive enough to study myelination in mice *in vivo*, and (2) to provide further evidence supporting the relationship between experience, myelination, and behaviour relative to sex in mice. This non-invasive imaging tool to detect

subtle differences in myelin *in vivo* is necessary for use in future studies using genetic mouse models and longitudinal deprivation-enrichment paradigms. These are required to better understand the role of myelination in development, experience-dependent adaptation, and psychiatric disorders.

Hypotheses:

1. The MTsat protocol will be sensitive enough to capture subtle hypomyelination in the PFC of socially isolated mice when compared to controls.
2. Socially isolated mice will show increased anxiogenic behaviour, decreased sociability, and decreased myelin content in the PFC.
3. Male mice will be more vulnerable to the deprivation paradigm than female mice, showing more pronounced differences in structure and behaviour.
4. Myelin quantification calculated using *ex vivo* histochemistry will correspond with the *in vivo* MRI findings.

3. Methodology

C57BL/6J mice originating from Jackson Laboratories (Bar Harbor, ME, USA) were bred in house to avoid the stress that transportation causes young animals, which could confound our results. All experimental mice were produced by six parent pairs. The mice were housed in a temperature- and humidity-controlled facility on a 12 hour light-dark cycle with *ad libitum* access to food and water. Cages were cleaned by veterinary staff every two weeks. C57BL/6J mice were specifically selected for this cross-sectional study because this strain was used to study SI induced myelin plasticity in adult mice (Liu et al., 2012), and to determine the critical

period for impactful SI in juvenile male mice (Makinodan et al., 2012). Behaviour data was collected for 60 mice (28 males) in each group. Of these, 48 mice were scanned (n = 12/group/sex). All procedures were carried out in accordance with the Canadian Council on Animal Care through the Montreal Neurological Institute Animal Care Committee.

3.1 Social Isolation Paradigm

At postnatal day (PN) 21, mice were weaned, ear-tagged, and housed either as social controls (3-4 mice per cage) or in isolation (1 mouse per cage) for two weeks. Cages were arranged vertically in the racks to impede visual contact with mice in other cages. Each cage received ventilated air to limit olfactory contact with other animals. All mice were handled by the same investigator for 5 minutes per mouse per day during the five days prior to PN 35 so that unexpected handling did not interfere with the results of behaviour experiments. Mice were weighed at PN 21 and again at PN 35. Starting at PN 35, behavioural tests and MRI scans were conducted 24 hours apart, beginning with Crawley's Sociability Test. This was followed by the Elevated-Zero Maze at PN 36, and the MRI at PN 37. Mice were then sacrificed and tissue was fixed on PN 38.

3.2 Behavioural Tests

Sociability and anxiogenic behaviour were measured using Crawley's Sociability Test and the Elevated-Zero Maze respectively. Between each trial, the apparatus was thoroughly cleaned with a 70% ethanol solution and Quatricide® to prevent olfactory cue bias and ensure proper sterilization. HVS Image, a camera-based computer tracking system, was used to score the path and time spent in the regions of interest in each test. All tests were performed in the morning, starting at approximately the same time. Animals were transported to the dimly-lit behaviour

room 30 minutes prior to the start of the experiment to acclimate. During each trial, mice were observed in silence from no less than two metres away from the apparatus.

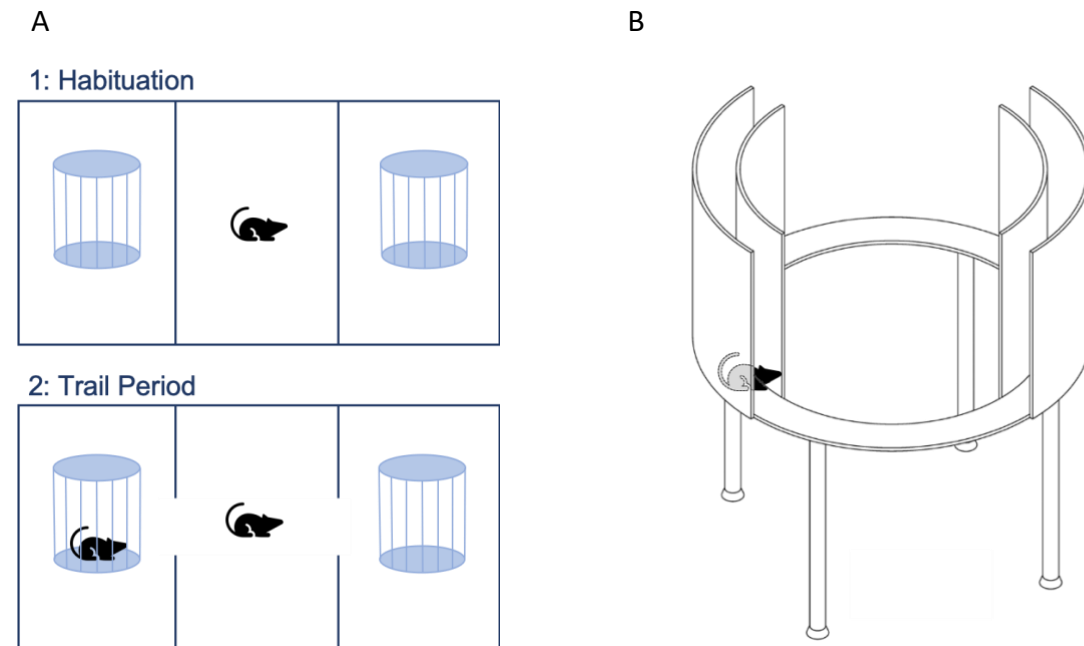


Figure 2: Behaviour test apparatus

a) Crawley's Sociability Test

b) Elevated 0 Maze, adapted from MazeEngineers, 2019

3.2.1 Crawley's Sociability Test

The three-chamber box (60 x 40 cm) has transparent plastic dividing walls with openings to provide free access between all three chambers (Figure 2a). There are identical vertical cages to hold intruder mice in each of the side chambers. This allows for air exchange, but limited direct physical interaction between the experimental and unfamiliar mice. The unfamiliar mice were the same strain, age, sex, and weight as the experimental mice. Each unfamiliar mouse was used for trials with multiple experimental mice.

The experimental mouse was habituated for five minutes in the centre of the empty three-chamber box. The unfamiliar mouse was then placed in one of the cages, alternating

sides between trials. The doors were removed to allow the experimental mouse to freely explore the chambers for ten minutes (Kaidanovich-Beilin, Lipina, Vukobradovic, Roder, & Woodgett, 2010). HVS Image video-tracking software was used to score approach-avoidance behaviours toward the unfamiliar mouse.

3.2.2 Elevated-Zero Maze

Anxiogenic behaviour was evaluated using the Elevated-Zero Maze. This maze is similar in concept to the conventional Elevated-Plus Maze, however its design eliminates the ambiguous area between the covered and uncovered arms. The elevated circular maze is divided into quadrants (Figure 2b). Two of these quadrants have raised walls that offer shelter, while the other two leave the mouse exposed. The experimental mouse was placed in one of the closed quadrants, alternating sides between trials. HVS Image video-tracking software tracked the mice as they explored the maze for five minutes. Number of line-crosses between quadrants, number and duration of entries into closed- and open-quadrants, and total locomotor activity were recorded.

3.3 Magnetic Resonance Imaging

Mice were transported by foot (500 m) in a covered and insulated cage to the McGill University and Genome Quebec Innovations Centre where the small bore 7 Tesla Bruker Pharmascan scanner is housed. The mice were awake during transportation, and were then scanned one at a time. Each mouse was placed in a sedation chamber with the isoflurane vaporizer at 4%, and the flowmeter at 300 ml/min. When the animal was recumbent, it was quickly transferred to the scanner room and positioned in a nosecone. Here, the flowmeter was set to 400 ml/min, and the isoflurane vaporizer was varied between 0.5-2% to maintain a stable

respiration rate of approximately 50 breaths per minute. Eye lubricant was applied and the mouse was gently secured to reduce motion artifacts in the images. Respiration and temperature were monitored, and the animal was warmed with air at 31°C. After the MRI protocol was complete, the mouse was placed on a hot water bottle in a separate cage for recovery.

Three 3D fast low angle shot (FLASH) images were acquired at 200 μ m isotropic resolution with three different contrasts to calculate T1 relaxation time, MTR and MTsat maps, to estimate brain tissue myelin content. T1 quantification was performed using a variable flip angle (VFA) protocol making use of FLASH images with proton density (PD)-weighted (FA = 5°, TR = 28ms), and T1-weighted contrast (FA = 25°, TR = 15ms) (Venkatesan, Lin, & Haacke, 1998). MTR and MTsat maps were calculated using the following scans: PD-weighted FLASH with and without a MT preparation module (gaussian pulse, 9.8 μ T, 8ms, 2 kHz) (Figure 3), and the above T1-weighted FLASH for MTsat (Helms et al., 2008). An interleaved multi-slice spin-echo echo planar imaging double-angle (EPI-DA) B1 mapping protocol (FA = 60°/180°, 120°/180°) was used for B1 correction of the T1 and MTsat maps (Boudreau et al., 2017).

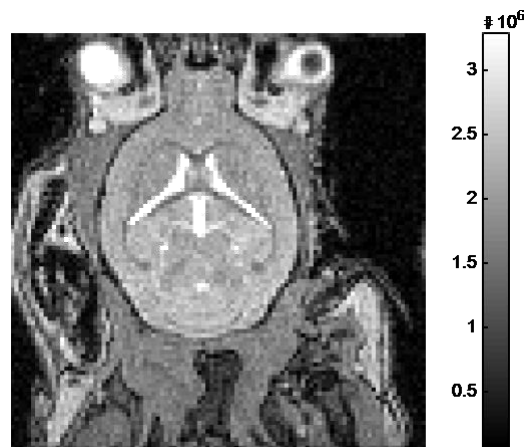


Figure 3: MT-weighted image of one mouse brain acquired using FLASH sequence

3.4 Tissue Fixation

At PN 38, the brains were fixed and prepared for either *ex vivo* MRI or immunofluorescence (IF). All mice were perfused with 4% paraformaldehyde (PFA) in 0.1M pH 7.4 phosphate buffered saline (PBS) at a rate of 10ml/min. For potential future work using *ex vivo* MRI, intact skulls were soaked overnight in the fixative solution at 4°C. They were then rinsed and stored in 0.01% sodium azide in 0.1M PBS at 4°C. For use in IF, brains were dissected from the skull, soaked in 30% sucrose solution overnight, flash-frozen in isopentane at -40°C, and stored at -80°C.

3.5 Immunofluorescence

Cryosectioning in preparation for IF was carried out on 12 mice that had previously been scanned; 6 in each condition (3 male). Due to the restraints put in place in response to COVID-19, the IF data were not collected and will instead be included in later work with the goal of validation MRI results. 20 µm coronal sections were cryosection cut onto superfrosted slides using optimal cutting temperature (OCT) embedding compound. Slides were stored frozen for future use. Staining protocol was established using practice slides with help from the Kennedy Lab (Figure 4). These slides were thawed for 1 hour, and rinsed in 0.1M PBS pH 7.4 to wash OCT. Sections were blocked for one hour with 5% normal goat heat inactivated serum with permeabilizing agent 0.5% Triton x100 (Fisher, in PBS). Sections were transferred to the primary antibodies with Triton x100 0.1%:

- Rabbit Iba-1: Ionizing calcium-binding adaptor molecule 1, expressed in microglia and macrophages (Imai, Ibata, Ito, Ohsawa, & Kohsaka, 1996)
- Mouse NeuN: Neuron-specific nuclear protein (Mullen, Buck, & Smith, 1992)

- Rat MBP: myelin-specific marker (Bodhireddy, Lyman, Rashbaum, & Weidenheim, 1994)

This was washed three times in the same block. Primary antibodies were detected using the appropriate secondary fluorescent antibodies (anti-rabbit, anti-mouse, anti-rat) and Deoxyribonucleic acid (DNA)-staining Hoechst 33342. Sections were thoroughly washed in PBS, mounted in immunogold, and dried overnight. Preliminary imaging was done on the Zeiss LSM 880 inverted confocal laser scanning microscope. Future analysis will be carried out using ImageJ.

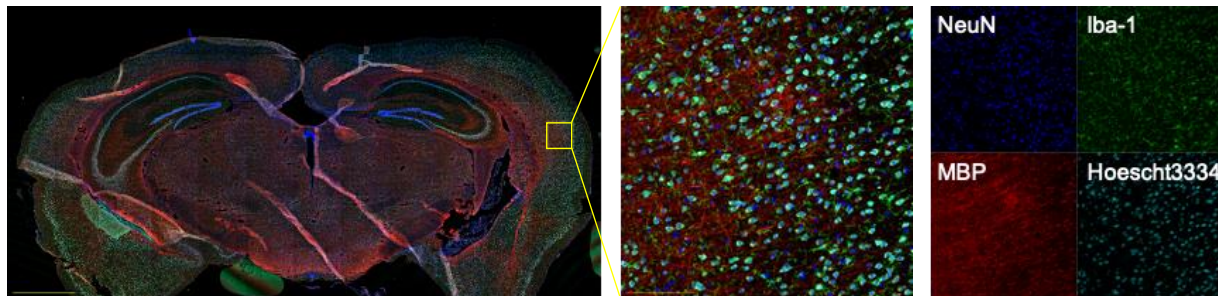


Figure 4: Sample images representing data to be acquired for histological validation of MRI results

3.6 Data Analysis

3.6.1 Image Processing

Analysis of the cross-sectional mouse MRI data was conducted in collaboration with Dr. Chakravarty's group, the Computational Brain Anatomy (CoBrA) Laboratory, as described in the group's previous publications (Chakravarty et al., 2015). MICe-build-model (MBM) is a multi-stage registration pipeline developed in the pydpiper framework (Friedel, van Eede, Pipitone, Mallar Chakravarty, & Lerch, 2014) that spatially aligns individual mouse brain imaging to a common space, the atlas (Dorr, Lerch, Spring, Kabani, & Henkelman, 2008; Richards et al., 2011; Steadman et al., 2014; Ullmann, Watson, Janke, Kurniawan, & Reutens, 1975), for subsequent analysis (van Eede, Scholz, Chakravarty, Henkelman, & Lerch, 2013). The Jacobian determinant

of the non-linear transformations to the common space are used in the whole-brain deformation based morphometry (DBM) analysis to detect local differences in brain volume between SI and control groups, and between males and females in each condition. MTR and MTsat images were also resampled into the common space for whole brain voxel-based analysis. Voxel-based and region of interest (ROI)-based statistics were carried out using R and RMINC. (Lerch, Hammill, van Eede, & Cassel, 2017)

3.6.2 Statistical Analysis

Assumption checks were performed using Shapiro-Wilk test for normality and Levene's test for homogeneity of variances. Student's t-tests and non-parametric Mann-Whitney U test for independent samples were used to identify group (SI or control) and sex differences in sociability and anxiogenic behaviour. Linear models and mixed effects models were used to further investigate fixed effects of group (SI or control) and sex, and the random effects of litter, parent pair, and weight gain on sociability and anxiogenic behaviour. For example, this model assumes an interaction between sex and group where ϵ is the error term:

$$\text{Behaviour} = \text{Sex} + \text{Group} + \text{Sex} * \text{Group} + (1 | \text{Litter}) + \epsilon$$

Additionally, the relationship between myelin content (indicated by MTsat and MTR) and behaviour was analysed:

$$\text{MTR} = \text{Sex} + \text{Group} + \text{Behaviour} + \epsilon$$

All statistical analyses were conducted using R.

4. Results

The final behaviour dataset included 33 controls (14 male), and 27 isolated mice (14 male). Of these mice, MRI scans were acquired for 48 mice; 24 in each condition (12 male).

4.1 Crawley's Sociability Test: No effect

Social interaction was measured as the percent of time spent in the chamber where the intruder mouse was housed, compared to the total time of the trial (10 minutes) (Figure 5a). These data meet assumptions of normality and homogeneity of variance. The Student's t-test revealed that social isolation had no effect on the sociability of male ($t(26) = 0.42, p = 0.68$) or female mice ($t(30) = 0.91, p = 0.37$) when compared to controls. Sex did not have an effect on social interaction ($t(58) = 0.35, p = 0.73$) (Figure 5b). No difference was observed in total path length between conditions or sexes (p 's > 0.07). Evaluation of linear models and mixed effects models revealed that anticipated random effects (litter, parent pair, weight gain, locomotor activity) did not play a significant role in the variability of sociability.

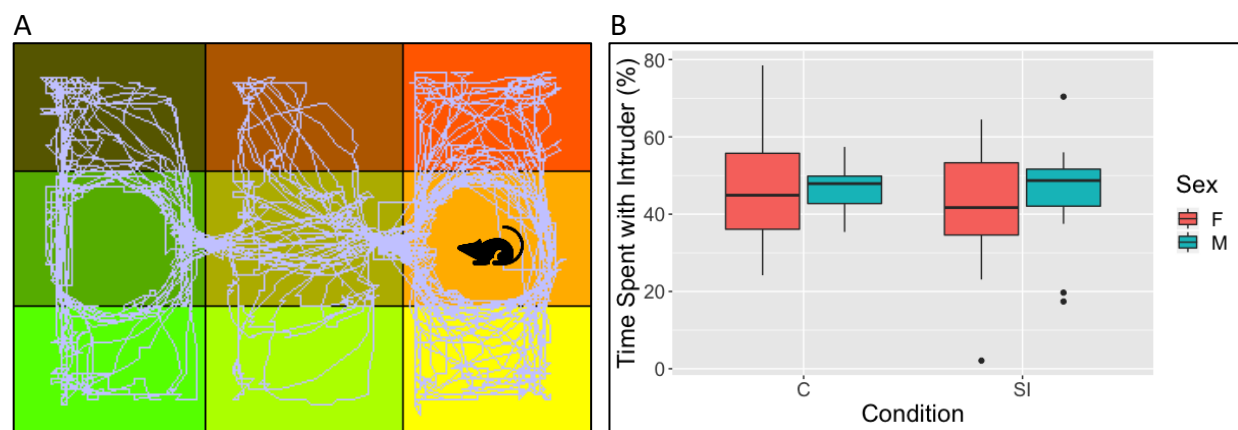


Figure 5: Sociability test results

a) Example of HVS Image tracking output is representative of the mean performance of male and female mice in either condition.

b) No difference was observed in the sociability behaviour for any of the groups ($M_{C_Male} = 46.9 \pm 6.0\%$; $M_{SI_Male} = 43.6 \pm 14.9\%$; $M_{C_Female} = 47.2 \pm 15.8\%$; $M_{SI_Female} = 41.9 \pm 16.4\%$).

4.2 Elevated-Zero Maze: Increased anxiogenic behaviour in males

Data from the Elevated-Zero maze was measured as the percent of time spent in the covered quadrants of the maze, compared to the total time of the trial (5 minutes) (Figure 6a).

This data was not normally distributed so the nonparametric Mann-Whitney U test for independent samples was used. Isolated male mice spent significantly more time in covered areas (Mdn = 89.6 %) compared to male controls (Mdn = 78.3 %) ($U = 46, p = 0.02$).

Interestingly, female mice showed no difference between conditions ($U = 128, p = 0.88$) (Figure 6b). No difference was observed in total path length between conditions or sexes (p 's > 0.11).

Evaluation of linear models and mixed effects models revealed that anticipated random effects (litter, parent pair, weight gain, locomotor activity) did not play a significant role in the variability observed in anxiogenic behaviour.

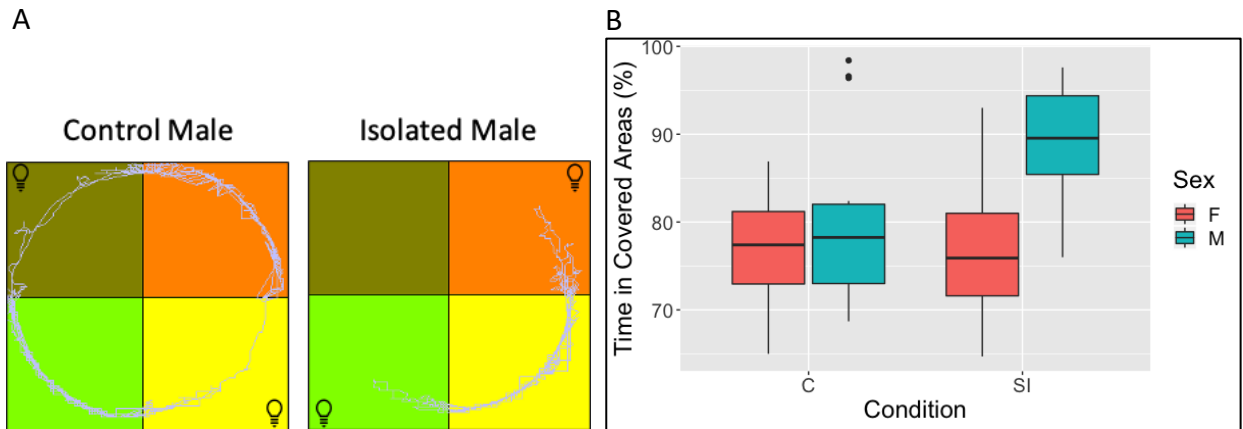


Figure 6: Anxiogenic behaviour test results

a) Examples of HVS Image tracking output represent average paths for control ($M = 79.9 \pm 9.7\%$) and isolated males ($M = 89.5 \pm 7.1\%$).

b) SI males showed significantly higher anxiety-like behaviours compared to controls. There was no difference observed between isolated and control females.

4.3 Imaging-based brain morphometry and microstructure

Deformation-based morphometry (DBM) analysis did not reveal any local anatomical differences between conditions. There were also no differences between groups in MTsat. This suggests that there is little to no SI-induced hypomyelination. Interestingly, MTR intensity was increased in isolated males compared to controls in the regions of the limbic stress circuit (Hipp and amygdala (AMG)), but not in the PFC as anticipated (Figure 7). There was no significant relationship between anxiogenic behaviour and MTR results.

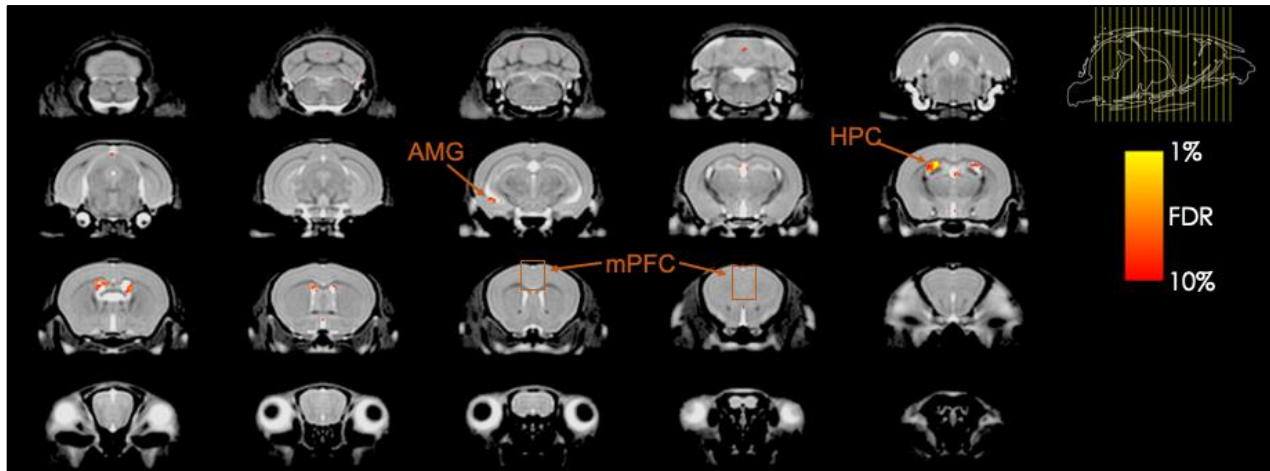


Figure 7: MTR results

Increased MTR in socially isolated male mice in comparison to controls ($n = 12$ per group) in regions of the limbic stress circuit (Hipp and AMG). The results are overlaid on the group average MT-weighted image.

5. Discussion

This project aimed to develop a non-invasive imaging tool capable of detecting subtle differences in myelin for use in establishing causality in the relationship between adaptive myelination and behaviour. MRI facilitates whole-brain image acquisition at multiple timepoints, which permits the use of the longitudinal paradigms and conditional knockout models needed to study causality and individual differences. Research indicates that social

isolation-induced subtle hypomyelination of the PFC in juvenile mice (Makinodan et al., 2012) can provide a platform to test myelin-sensitive MT imaging. This pilot project has effectively provided a foundation upon which we can build and expand in the future.

5.1 No Difference in Sociability

The lack of difference in sociability falls within the realm of possible outcomes. In previous research, SI led to increased sociability (Matthews et al., 2016), decreased sociability (Liu et al., 2012; Makinodan et al., 2017, 2012; Okada et al., 2015), and no change in sociability (Pais et al., 2019). While most studies used only male mice, the ones that included females as well showed both similar (Liu et al., 2012) and differential results between the sexes (Medendorp et al., 2018; Pais et al., 2019). It is important to note that direct comparisons cannot be made between these studies because influential factors such as age at isolation and testing, duration of isolation, and mouse strain differ.

In a recent study, four inbred mouse strains were used to investigate the impact of genetic background on response to a chronic psychosocial stressor. Differences between the strains were observed in resilience, behaviour, ODC gene expression, and myelin thickness. Interestingly, C57BL/6NCrl mice, a substrain similar to C57BL/6J, were significantly more resilient to the chronic stressor than other wildtype strains (Laine et al., 2018). This indicates the need to evaluate strain differences in vulnerability to SI specifically, and demonstrates the overarching effect of genetics on adaptive myelination and behaviour. With this in mind, it follows that we should have observed the decrease in sociability seen in other studies using C57BL/6J mice (Liu et al., 2012; Makinodan et al., 2012). The fact that there was no difference suggests that the two-week SI paradigm may not have been long enough to affect PFC

functioning and resulting behaviour. Alternatively, factors such as breeding in-house rather than shipment of young animals may factor into the increased resilience observed.

5.2 Elevated Anxiogenic Behaviour in Isolated Males

The finding that isolated male mice show heightened anxiogenic behaviour in the Elevated-Zero maze corresponds with previous SI literature (Amiri et al., 2015; Fone & Porkess, 2008; Lander et al., 2017). The lack of change in female anxiety-like behaviour mirrors studies showing that females are more resilient to SI. (Lukkes, Watt, Lowry, & Forster, 2009; Rodgers & Cole, 1993; Weiss, Pryce, Jongen-Rêlo, Nanz-Bahr, & Feldon, 2004).

It is also possible that female mice are not susceptible to SI during the same critical period that was established in males. A longitudinal study using MRI to follow mouse brain development across nine timepoints from infancy to adulthood demonstrated elaborate differences in volume and developmental trajectory between sexes. Interestingly, brain regions that are larger in males tend to develop earlier in males than in females, with differences emerging before puberty (PN 27 ± 2 in males, PN 32 ± 3 in females) (Qiu et al., 2018). Such areas include the AMG and Hipp, the regions where elevated MTR signal was observed in isolated males and not females in the present study. While the neuroanatomical volume studied by Qiu *et al.* is not indicative of myelination, the fact that neurodevelopmental stages differ between sexes is relevant in identifying a universal critical period of sensitivity to SI. It would be a valuable contribution to knowledge to apply the MRI protocol developed in this project to conduct a longitudinal study similar to Qiu *et al.*'s investigating the normal developmental trajectory of myelination in mice with respect to sex.

5.3 Increased MTR in Limbic System

There was no difference detected in MTsat or brain morphology between conditions. This indicates that the MTsat protocol was not sensitive enough to capture any minute myelin differences. Increased MTR was observed in regions of the AMG and Hipp in isolated male mice. These limbic areas play an important role in the stress response, which is activated by SI in rodents (Lukkes et al., 2009; Weiss et al., 2004). The AMG, Hipp, and PFC regulate the stress response by exerting control over the hypothalamic-pituitary-adrenal (HPA) axis. Top-down control of the HPA stress axis primarily comes from the medial PFC and Hipp via inhibitory GABAergic inputs, while excitatory glutamatergic signalling is released from the AMG (Fone & Porkess, 2008; Maguire & Salpekar, 2013). In a healthy brain, inhibitory and excitatory signalling are balanced and allows for the animal to accurately interpret and respond to the stressor. In the case of many chronic stressors such as SI, this equilibrium can become destabilized leaving the animal hypersensitive to any future stress it may experience.

The observed increase in MTR in the limbic areas in SI males could be explained by activity-dependent increases in myelination. In 2014, Gibson *et al.* used optogenetics to demonstrate that neuronal activation can stimulate the proliferation of oligodendrocyte progenitor cells which leads to an increased number of ODCs and myelin sheath thickening. These physiological modifications are accompanied by adaptive changes in behaviour (Gibson et al., 2014). In the present study, increased myelination in the AMG and Hipp may be a result of SI-induced hyperactivation of the neurons in the HPA-axis and surrounding circuitry (Lukkes et al., 2009; Weiss et al., 2004). The finding that MTR is increased in limbic regions in isolated male mice corresponds theoretically with the observed increase in anxiogenic behaviour in the

same cohort, however there was no significant relationship between behaviour and MRI results. This lack of correlation is not uncommon in similar studies (Schubert, Porkess, Dashdorj, Fone, & Auer, 2009).

MT imaging assumes that most macromolecular content in the CNS is myelin. MTR is more susceptible to T1 confounds than MTsat, meaning that it is less specific to myelin (Heath et al., 2018). Inflammation (Gareau, Rutt, Karlik, & Mitchell, 2000) and immune response (Blezer, Bauer, Brok, Nicolay, & 't Hart, 2007) can impact signal intensity in MTR, and are influenced by dysregulation of the limbic-HPA-axis (Lozovaya & Miller, 2003). The immunohistochemistry protocol was developed in order to establish whether the increases in MTR can be explained by myelin (MBP), or inflammation (microglia and macrophages expressing Iba-1). When complete, these data will offer the validation necessary for the next steps of this project.

5.4 Limitations

This study aimed to replicate Makinodan *et al.*'s finding that isolation during the critical period between PN 21 and 35 induces hypomyelination in the PFC of mice and related behavioural deficits (Makinodan et al., 2012), and to capture this hypomyelination *in vivo* using quantitative MRI. Despite best efforts, this was not the case. The success of this study was most likely limited by the age of the mice. Behaviour tests have largely been validated in adult male mice, however in this study we use early-adolescent males and females. For example, young mice interact through social play and show more prosocial behaviours than adults. This difference is especially pronounced in males (Bell et al., 2010). For this reason, the social

interaction test may not be an effective measure of sociability because it is based on the social tendencies of more aggressive adult mice.

Additionally, brain size, and therefore age, affects the ability of MRI to capture subtle differences in myelination. The resolution limits our ability to capture differences in small structures, but this is not the case for the PFC. Brain size impacts the signal-to-noise ratio of the images acquired due to the coil fill factor. Finally, the brains of younger mice may be less myelinated limiting the potential contrast available to detect. In Poggi's study using MT imaging to detect subtle changes in myelination, the mice were 6 and 18 months old (Poggi et al., 2016). Total brain volume continues to increase from adolescence into adulthood (Qiu et al., 2018). In order to image mice when they are older and possibly increase the myelin deficit, a prolonged isolation period can be implemented. If mice are isolated for four weeks starting at PN 21, the critical period is captured, while allowing mice to mature further. This design would also increase the validity of the behaviour tests for use in this population.

The results may have been impacted by differences in animal handling practices, as the Makinodan group did not specify their methods (Makinodan et al., 2017, 2012). This well-known confound has been shown to impact the outcomes of various behaviour tests and biological measures (Ghosal et al., 2015; Gouveia & Hurst, 2017). Further, it is worthwhile to note that the estrous cycle was not controlled for in female mice. Repeated smear testing acts as an additional stressor for females, potentially stimulating the HPA-axis, and introducing a sex-related confound (Pietropaolo et al., 2008).

6. Conclusion

In rodents, sociability is more directly related to PFC hypomyelination than anxiogenic behaviour is (Poggi et al., 2016). Increased anxiogenic behaviour can be produced by the inability of the PFC to exert top-down control over the HPA-axis. However, hyper- or hypo-activity in other limbic regions (AMG, Hipp) can also lead to the disequilibrium of the stress circuitry (Herman, Ostrander, Mueller, & Figueiredo, 2005). In this project, it is likely that SI elicited an imbalance in HPA-axis activation through a cascade of events other than PFC hypomyelination. This may explain why sociability was unaffected when anxiogenic behaviour was increased in males. The histological validation of the MRI data is necessary to proceed with future research.

Next steps include implementing a prolonged SI paradigm in order to determine whether the impact of SI is a dose-dependent interaction. The MRI protocol can be used for imaging myelin content at multiple timepoints to evaluate the dynamic spectrum of adaptive myelination. Conditional knockout models can be used to continue to work towards establishing causality in the relationship between adaptive myelination and behaviour.

References

- Agoglia, A. E., Holstein, S. E., Small, A. T., Spanos, M., Burrus, B. M., & Hodge, C. W. (2017). Comparison of the adolescent and adult mouse prefrontal cortex proteome. *PLoS ONE*, *12*(6). <https://doi.org/10.1371/journal.pone.0178391>
- Amiri, S., Haj-Mirzaian, A., Amini-khoei, H., Momeny, M., Shirzadian, A., Balaei, M. R., ... Mehr, S. E. (2016). NMDA receptor antagonists attenuate the proconvulsant effect of juvenile social isolation in male mice. *Brain Research Bulletin*, *121*, 158–168. <https://doi.org/10.1016/j.brainresbull.2016.01.013>
- Amiri, S., Haj-Mirzaian, A., Rahimi-balaei, M., Razmi, A., Kordjazy, N., Shirzadian, A., ... Dehpour, A. R. (2015). Co-occurrence of anxiety and depressive-like behaviors following adolescent social isolation in male mice; possible role of nitrenergic system. *Physiology and Behavior*, *145*, 38–44. <https://doi.org/10.1016/j.physbeh.2015.03.032>
- Andersen, S. L., & Teicher, M. H. (2008, April). Stress, sensitive periods and maturational events in adolescent depression. *Trends in Neurosciences*. <https://doi.org/10.1016/j.tins.2008.01.004>
- Aswendt, M., Adamczak, J., & Tennstaedt, A. (2014). A review of novel optical imaging strategies of the stroke pathology and stem cell therapy in stroke. *Frontiers in Cellular Neuroscience*, *8*, 226. <https://doi.org/10.3389/fncel.2014.00226>
- Bangasser, D. A., & Valentino, R. J. (2014). Sex differences in stress-related psychiatric disorders: Neurobiological perspectives. <https://doi.org/10.1016/j.yfrne.2014.03.008>
- Baraban, M., Mensch, S., & Lyons, D. A. (2016). Adaptive myelination from fish to man. *Brain Research*. <https://doi.org/10.1016/j.brainres.2015.10.026>
- Bell, H. C., Pellis, S. M., & Kolb, B. (2010). Juvenile peer play experience and the development of the orbitofrontal and medial prefrontal cortices. *Behavioural Brain Research*, *207*(1), 7–13. <https://doi.org/10.1016/j.bbr.2009.09.029>
- Bengtsson, S. L., Nagy, Z., Skare, S., Forsman, L., Forssberg, H., & Ullén, F. (2005). Extensive piano practicing has regionally specific effects on white matter development. *Nature Neuroscience*, *8*(9), 1148–1150. <https://doi.org/10.1038/nn1516>
- Bin, J. M., & Lyons, D. A. (2016). Imaging Myelination In Vivo Using Transparent Animal Models.

- Brain Plasticity*, 2(1), 3–29. <https://doi.org/10.3233/bpl-160029>
- Blezer, E. L. A., Bauer, J., Brok, H. P. M., Nicolay, K., & 't Hart, B. A. (2007). Quantitative MRI-pathology correlations of brain white matter lesions developing in a non-human primate model of multiple sclerosis. *NMR in Biomedicine*, 20(2), 90–103. <https://doi.org/10.1002/nbm.1085>
- Bodhireddy, S. R., Lyman, W. D., Rashbaum, W. K., & Weidenheim, K. M. (1994). Immunohistochemical detection of myelin basic protein is a sensitive marker of myelination in second trimester human fetal spinal cord. *Journal of Neuropathology and Experimental Neurology*, 53(2), 144–149. <https://doi.org/10.1097/00005072-199403000-00005>
- Boudreau, M., Tardif, C. L., Stikov, N., Sled, J. G., Lee, W., & Pike, G. B. (2017). B1 mapping for bias-correction in quantitative T1 imaging of the brain at 3T using standard pulse sequences. *Journal of Magnetic Resonance Imaging*, 46(6), 1673–1682. <https://doi.org/10.1002/jmri.25692>
- Boullerne, A. I. (2016, September). The history of myelin. *Experimental Neurology*. NIH Public Access. <https://doi.org/10.1016/j.expneurol.2016.06.005>
- Bunge, M. B., Bunge, R. P., & Pappas, G. D. (1962). Electron microscopic demonstration of connections between glia and myelin sheaths in the developing mammalian central nervous system. *The Journal of Cell Biology*, 12(2), 448–453. <https://doi.org/10.1083/jcb.12.2.448>
- Bunge, R. (1968). Glial cells and the central myelin sheath. *Physiological Reviews*, 48(1), 197–251. <https://doi.org/10.1152/physrev.1968.48.1.197>
- Cajal, S. R. (1912). El aparato endocelular de Golgi de la célula de Schwann y algunas observaciones sobre la estructura de los tubos nerviosos. *Trabajos Del Laboratorio de Investigaciones Biológicas de La Universidad de Madrid*, 10, 221–246.
- Chadda, R., & Devaud, L. L. (2004). Sex differences in effects of mild chronic stress on seizure risk and GABAA receptors in rats. In *Pharmacology Biochemistry and Behavior* (Vol. 78, pp. 495–504). <https://doi.org/10.1016/j.pbb.2004.03.022>
- Chakravarty, M. M., Nobrega, J. N., Lerch, J. P., Laliberté, C., Lozano, A. M., Martinez-Canabal,

- A., ... Lerch, J. P. (2015). Deep brain stimulation of the ventromedial prefrontal cortex causes reorganization of neuronal processes and vasculature. *NeuroImage*, *125*, 422–427. <https://doi.org/10.1016/j.neuroimage.2015.10.049>
- Chang, C. H., Hsiao, Y. H., Chen, Y. W., Yu, Y. J., & Gean, P. W. (2015). Social isolation-induced increase in NMDA receptors in the hippocampus exacerbates emotional dysregulation in mice. *Hippocampus*, *25*(4), 474–485. <https://doi.org/10.1002/hipo.22384>
- Chapman, T. W., & Hill, R. A. (2020, January 10). Myelin plasticity in adulthood and aging. *Neuroscience Letters*. Elsevier Ireland Ltd. <https://doi.org/10.1016/j.neulet.2019.134645>
- Chen, H. J. C., Spiers, J. G., Sernia, C., & Lavidis, N. A. (2015). Response of the nitrenergic system to activation of the neuroendocrine stress axis. *Frontiers in Neuroscience*. Frontiers Media S.A. <https://doi.org/10.3389/fnins.2015.00003>
- Chugani, H. T., Behen, M. E., Muzik, O., Juhász, C., Nagy, F., & Chugani, D. C. (2001). Local brain functional activity following early deprivation: A study of postinstitutionalized Romanian orphans. *NeuroImage*, *14*(6), 1290–1301. <https://doi.org/10.1006/nimg.2001.0917>
- Dawson, M. R. L., Polito, A., Levine, J. M., & Reynolds, R. (2003). NG2-expressing glial progenitor cells: An abundant and widespread population of cycling cells in the adult rat CNS. *Molecular and Cellular Neuroscience*, *24*(2), 476–488. [https://doi.org/10.1016/S1044-7431\(03\)00210-0](https://doi.org/10.1016/S1044-7431(03)00210-0)
- De Villers-Sidani, E., Chang, E. F., Bao, S., & Merzenich, M. M. (2007). Critical period window for spectral tuning defined in the primary auditory cortex (A1) in the rat. *Journal of Neuroscience*, *27*(1), 180–189. <https://doi.org/10.1523/JNEUROSCI.3227-06.2007>
- Deber, C. M., & Reynolds, S. J. (1991). Central nervous system myelin: structure, function, and pathology. *Clinical Biochemistry*. [https://doi.org/10.1016/0009-9120\(91\)90421-A](https://doi.org/10.1016/0009-9120(91)90421-A)
- del Río-Hortega, P. (1921). Estudios sobre la neurologia. La glía de escasas radiaciones (oligodendroglía). *Boletín de La Real Sociedad Española de Historia Natural*, *21*, 63–92.
- Dorr, A. E., Lerch, J. P., Spring, S., Kabani, N., & Henkelman, R. M. (2008). High resolution three-dimensional brain atlas using an average magnetic resonance image of 40 adult C57Bl/6J mice. <https://doi.org/10.1016/j.neuroimage.2008.03.037>
- Ferdman, N., Murmu, R. P., Bock, J., Braun, K., & Leshem, M. (2007). Weaning age, social

- isolation, and gender, interact to determine adult explorative and social behavior, and dendritic and spine morphology in prefrontal cortex of rats. *Behavioural Brain Research*, *180*(2), 174–182. <https://doi.org/10.1016/j.bbr.2007.03.011>
- Fields, R. D. (2015). A new mechanism of nervous system plasticity: activity-dependent myelination. *Nature Reviews. Neuroscience*, *16*(12), 756–767. <https://doi.org/10.1038/nrn4023>
- Fields, R. D., Araque, A., Johansen-Berg, H., Lim, S. S., Lynch, G., Nave, K. A., ... Wake, H. (2014). Glial biology in learning and cognition. *Neuroscientist*, *20*(5), 426–431. <https://doi.org/10.1177/1073858413504465>
- Fone, K. C. F., & Porkess, M. V. (2008, August). Behavioural and neurochemical effects of post-weaning social isolation in rodents-Relevance to developmental neuropsychiatric disorders. *Neuroscience and Biobehavioral Reviews*. <https://doi.org/10.1016/j.neubiorev.2008.03.003>
- Fralix, T. A., Ceckler, T. L., Wolff, S. D., Simon, S. A., & Balaban, R. S. (1991). Lipid bilayer and water proton magnetization transfer: Effect of cholesterol. *Magnetic Resonance in Medicine*, *18*(1), 214–223. <https://doi.org/10.1002/mrm.1910180122>
- Friedel, M., van Eede, M. C., Pipitone, J., Mallar Chakravarty, M., & Lerch, J. P. (2014). Pydpipe: A flexible toolkit for constructing novel registration pipelines. *Frontiers in Neuroinformatics*, *8*(JULY), 67. <https://doi.org/10.3389/fninf.2014.00067>
- Gareau, P. J., Rutt, B. K., Karlik, S. J., & Mitchell, J. R. (2000). Magnetization transfer and multicomponent T2 relaxation measurements with histopathologic correlation in an experimental model of MS. *Journal of Magnetic Resonance Imaging*, *11*(6), 586–595. [https://doi.org/10.1002/1522-2586\(200006\)11:6<586::AID-JMRI3>3.0.CO;2-V](https://doi.org/10.1002/1522-2586(200006)11:6<586::AID-JMRI3>3.0.CO;2-V)
- Ghosal, S., Nunley, A., Mahbod, P., Lewis, A. G., Smith, E. P., Tong, J., ... Herman, J. P. (2015). Mouse handling limits the impact of stress on metabolic endpoints. *Physiology and Behavior*, *150*, 31–37. <https://doi.org/10.1016/j.physbeh.2015.06.021>
- Gibson, E. M., Purger, D., Mount, C. W., Goldstein, A. K., Lin, G. L., Wood, L. S., ... Monje, M. (2014). Neuronal activity promotes oligodendrogenesis and adaptive myelination in the mammalian brain. *Science*, *344*(6183). <https://doi.org/10.1126/science.1252304>

- Gouveia, K., & Hurst, J. L. (2017). Optimising reliability of mouse performance in behavioural testing: The major role of non-aversive handling. *Scientific Reports*, 7(1), 1–12.
<https://doi.org/10.1038/srep44999>
- Haj-Mirzaian, A., Amiri, S., Amini-Khoei, H., Rahimi-Balaei, M., Kordjazy, N., Olson, C. O., ... Mehr, S. E. (2016). Attenuation of oxidative and nitrosative stress in cortical area associates with antidepressant-like effects of tropisetron in male mice following social isolation stress. *Brain Research Bulletin*, 124, 150–163.
<https://doi.org/10.1016/j.brainresbull.2016.04.018>
- Heath, F., Hurley, S. A., Johansen-Berg, H., & Sampaio-Baptista, C. (2018). Advances in Noninvasive Myelin Imaging. *Develop Neurobiol*, 78, 136–151.
<https://doi.org/10.1002/dneu.22552>
- Helms, G., Dathe, H., Kallenberg, K., & Dechent, P. (2008). High-resolution maps of magnetization transfer with inherent correction for RF inhomogeneity and T1 relaxation obtained from 3D FLASH MRI. *Magnetic Resonance in Medicine*, 60(6), 1396–1407.
<https://doi.org/10.1002/mrm.21732>
- Herman, J. P., Ostrander, M. M., Mueller, N. K., & Figueiredo, H. (2005, December 1). Limbic system mechanisms of stress regulation: Hypothalamo-pituitary- adrenocortical axis. *Progress in Neuro-Psychopharmacology and Biological Psychiatry*. Elsevier.
<https://doi.org/10.1016/j.pnpbp.2005.08.006>
- Hinton, E. A., Li, D. C., Allen, A. G., & Gourley, S. L. (2019). Social isolation in adolescence disrupts cortical development and goal-dependent decision-making in adulthood, despite social reintegration. *ENeuro*, 6(5). <https://doi.org/10.1523/ENEURO.0318-19.2019>
- Hortega, P. R. (1928). *Tercera aportación al conocimiento morfológico e interpretación funcional de la oligodendroglia*. Museo Nacional de Ciencias Naturales. Retrieved from <https://books.google.ca/books?id=fcO3MwEACAAJ>
- Hudson, L. D. (2003). Pelizaeus-Merzbacher disease and spastic paraplegia type 2: Two faces of myelin loss from mutations in the same gene. *Journal of Child Neurology*, 18(9), 616–624.
<https://doi.org/10.1177/08830738030180090801>
- Imai, Y., Ibata, I., Ito, D., Ohsawa, K., & Kohsaka, S. (1996). A novel gene iba1 in the major

- histocompatibility complex class III region encoding an EF hand protein expressed in a monocytic lineage. *Biochemical and Biophysical Research Communications*, 224(3), 855–862. <https://doi.org/10.1006/bbrc.1996.1112>
- Kaidanovich-Beilin, O., Lipina, T., Vukobradovic, I., Roder, J., & Woodgett, J. R. (2010). Assessment of social interaction behaviors. *Journal of Visualized Experiments*. <https://doi.org/10.3791/2473>
- Kaller, M. S., Lazari, A., Blanco-Duque, C., Sampaio-Baptista, C., & Johansen-Berg, H. (2017, December 1). Myelin plasticity and behaviour — connecting the dots. *Current Opinion in Neurobiology*. Elsevier Current Trends. <https://doi.org/10.1016/j.conb.2017.09.014>
- Kandel, E. R., Schwartz, J. H., Jessell, T. M., Siegelbaum, S. A., & Hudspeth, A. J. (2013). *Principles of Neural Science* (5th ed.). McGraw-Hill Companies.
- Kawasaki, T., Ago, Y., Yano, K., Araki, R., Washida, Y., Onoe, H., ... Matsuda, T. (2011). Increased binding of cortical and hippocampal group II metabotropic glutamate receptors in isolation-reared mice. *Neuropharmacology*, 60(2–3), 397–404. <https://doi.org/10.1016/j.neuropharm.2010.10.009>
- Kettenmann, H., & Ransom, B. R. (2013). The Concept of Neuroglia: A Historical Perspective. In *Neuroglia* (pp. 1–16). Oxford University Press. <https://doi.org/10.1093/acprof:oso/9780195152227.003.0001>
- Laine, M. A., Trontti, K., Misiewicz, Z., Sokolowska, E., Kuleskaya, N., Heikkinen, A., ... Hovatta, I. (2018). Genetic control of myelin plasticity after chronic psychosocial stress. *ENeuro*, 5(4), 166–184. <https://doi.org/10.1523/ENEURO.0166-18.2018>
- Lander, S. S., Linder-Shacham, D., & Gaisler-Salomon, I. (2017). Differential effects of social isolation in adolescent and adult mice on behavior and cortical gene expression. *Behavioural Brain Research*, 316, 245–254. <https://doi.org/10.1016/j.bbr.2016.09.005>
- Lerch, J. P., Hammill, C., van Eede, M. C., & Cassel, D. (2017). RMINC: Statistical Tools for Medical Imaging NetCDF (MINC) Files. R package version 1.5.2.1. Retrieved from <http://mouse-imaging-centre.github.io/RMINC>.
- Levitt, P. (2003). Structural and functional maturation of the developing primate brain. In *Journal of Pediatrics* (Vol. 143, pp. 35–45). Mosby Inc. <https://doi.org/10.1067/s0022->

3476(03)00400-1

Lim, A. L., Taylor, D. A., & Malone, D. T. (2011). Isolation rearing in rats: Effect on expression of synaptic, myelin and GABA-related immunoreactivity and its utility for drug screening via the subchronic parenteral route. *Brain Research*, *1381*, 52–65.

<https://doi.org/10.1016/J.BRAINRES.2011.01.017>

Lister, J. J. (1830). XIII. On some properties in achromatic object-glasses applicable to the improvement of the microscope. *Philosophical Transactions of the Royal Society of London*, *120*, 187–200. <https://doi.org/10.1098/rstl.1830.0015>

Liu, J., Dietz, K., Deloyht, J. M., Pedre, X., Kelkar, D., Kaur, J., ... Casaccia, P. (2012). Impaired adult myelination in the prefrontal cortex of socially isolated mice. *Nature Neuroscience*, *15*(12), 1621–1623. <https://doi.org/10.1038/nn.3263>

Lozovaya, N., & Miller, A. D. (2003, June 6). Chemical neuroimmunology: Health in a nutshell bidirectional communication between immune and stress (limbic-hypothalamic-pituitary-adrenal) systems. *ChemBioChem*. John Wiley & Sons, Ltd.

<https://doi.org/10.1002/cbic.200200492>

Lukkes, J. L., Watt, M. J., Lowry, C. A., & Forster, G. L. (2009). Consequences of post-weaning social isolation on anxiety behavior and related neural circuits in rodents. *Frontiers in Behavioral Neuroscience*, *3*(AUG), 1–12. <https://doi.org/10.3389/neuro.08.018.2009>

Maes, M., Galecki, P., Chang, Y. S., & Berk, M. (2011, April 29). A review on the oxidative and nitrosative stress (O&NS) pathways in major depression and their possible contribution to the (neuro)degenerative processes in that illness. *Progress in Neuro-Psychopharmacology and Biological Psychiatry*. <https://doi.org/10.1016/j.pnpbp.2010.05.004>

Maguire, J., & Salpekar, J. A. (2013, March). Stress, seizures, and hypothalamic-pituitary-adrenal axis targets for the treatment of epilepsy. *Epilepsy and Behavior*.

<https://doi.org/10.1016/j.yebeh.2012.09.040>

Makinodan, M., Kimoto, S., Komori, T., Kanba, S., Yoshino, H., Okumura, K., ... Fukami, S. (2017). Effects of the mode of re-socialization after juvenile social isolation on medial prefrontal cortex myelination and function. *Scientific Reports*, *7*(1), 1–9.

<https://doi.org/10.1038/s41598-017-05632-2>

- Makinodan, M., Rosen, K. M., Ito, S., & Corfas, G. (2012). A Critical Period for Social Experience-dependent Oligodendrocyte Maturation and Myelination. *Science*, *337*(6100), 1357–1360. <https://doi.org/10.1126/science.1220845>.A
- Matsumoto, K., Fujiwara, H., Araki, R., & Yabe, T. (2019, November 1). Post-weaning social isolation of mice: A putative animal model of developmental disorders. *Journal of Pharmacological Sciences*. Japanese Pharmacological Society. <https://doi.org/10.1016/j.jpsh.2019.10.002>
- Matsumoto, K., Puia, G., Dong, E., & Pinna, G. (2007, January 7). GABAA receptor neurotransmission dysfunction in a mouse model of social isolation-induced stress: Possible insights into a non-serotonergic mechanism of action of SSRIs in mood and anxiety disorders. *Stress*. <https://doi.org/10.1080/10253890701200997>
- Matthews, G. A., Nieh, E. H., Vander Weele, C. M., Halbert, S. A., Pradhan, R. V., Yosafat, A. S., ... Tye, K. M. (2016). Dorsal Raphe Dopamine Neurons Represent the Experience of Social Isolation. *Cell*, *164*(4), 617–631. <https://doi.org/10.1016/j.cell.2015.12.040>
- McRobbie, D. W., Moore, E. A., Graves, M. J., & Prince, M. R. (2006). *MRI from picture to proton. MRI from Picture to Proton*. Cambridge: Cambridge University Press. <https://doi.org/10.1017/CBO9780511545405>
- Medendorp, W. E., Petersen, E. D., Pal, A., Wagner, L. M., Myers, A. R., Hochgeschwender, U., & Jenrow, K. A. (2018). Altered behavior in mice socially isolated during adolescence corresponds with immature dendritic spine morphology and impaired plasticity in the prefrontal cortex. *Frontiers in Behavioral Neuroscience*, *12*, 87. <https://doi.org/10.3389/fnbeh.2018.00087>
- Mullen, R. J., Buck, C. R., & Smith, A. M. (1992). NeuN, a neuronal specific nuclear protein in vertebrates. *Development*, *116*(1), 201–211.
- Murínová, J., Hlaváčová, N., Chmelová, M., & Riečanský, I. (2017, May 31). The evidence for altered BDNF expression in the brain of rats reared or housed in social isolation: A systematic review. *Frontiers in Behavioral Neuroscience*. Frontiers Media S.A. <https://doi.org/10.3389/fnbeh.2017.00101>
- Nave, K.-A., & Trapp, B. D. (2008). Axon-Glial Signaling and the Glial Support of Axon Function.

- Annual Review of Neuroscience*, 31(1), 535–561.
<https://doi.org/10.1146/annurev.neuro.30.051606.094309>
- Norton, W. T., & Poduslo, S. E. (1973). Myelination in rat brain: method of myelin isolation. *Journal of Neurochemistry*, 21(4), 749–757. <https://doi.org/10.1111/j.1471-4159.1973.tb07519.x>
- Okada, R., Fujiwara, H., Mizuki, D., Araki, R., Yabe, T., & Matsumoto, K. (2015). Involvement of dopaminergic and cholinergic systems in social isolation-induced deficits in social affiliation and conditional fear memory in mice. *Neuroscience*, 299, 134–145.
<https://doi.org/10.1016/j.neuroscience.2015.04.064>
- Pais, A. B., Pais, A. C., Elmisurati, G., Park, S. H., Miles, M. F., & Wolstenholme, J. T. (2019). A novel neighbor housing environment enhances social interaction and rescues cognitive deficits from social isolation in adolescence. *Brain Sciences*, 9(12), 336.
<https://doi.org/10.3390/brainsci9120336>
- Pajevic, S., Basser, P. J., & Fields, R. D. (2014). Role of myelin plasticity in oscillations and synchrony of neuronal activity. *Neuroscience*, 276, 135–147.
<https://doi.org/10.1016/j.neuroscience.2013.11.007>
- Palanza, P. (2001). Animal models of anxiety and depression: How are females different? *Neuroscience and Biobehavioral Reviews*, 25(3), 219–233. [https://doi.org/10.1016/S0149-7634\(01\)00010-0](https://doi.org/10.1016/S0149-7634(01)00010-0)
- Palanza, P., Gioiosa, L., & Parmigiani, S. (2001). Social stress in mice: Gender differences and effects of estrous cycle and social dominance. *Physiology and Behavior*, 73(3), 411–420.
[https://doi.org/10.1016/S0031-9384\(01\)00494-2](https://doi.org/10.1016/S0031-9384(01)00494-2)
- Paus, T., Collins, D. L., Evans, A. C., Leonard, G., Pike, B., & Zijdenbos, A. (2001). Maturation of white matter in the human brain: A review of magnetic resonance studies. *Brain Research Bulletin*, 54(3), 255–266. [https://doi.org/10.1016/S0361-9230\(00\)00434-2](https://doi.org/10.1016/S0361-9230(00)00434-2)
- Penfield, W. (1924). Oligodendroglia and its relation to classical neuroglia. *Brain*, 47(4), 430–452. <https://doi.org/10.1093/brain/47.4.430>
- Pietropaolo, S., Singer, P., Feldon, J., & Yee, B. K. (2008). The postweaning social isolation in C57BL/6 mice: Preferential vulnerability in the male sex. *Psychopharmacology*, 197(4),

- 613–628. <https://doi.org/10.1007/s00213-008-1081-3>
- Poggi, G., Boretius, S., Möbius, W., Moschny, N., Baudewig, J., Ruhwedel, T., ... Ehrenreich, H. (2016). Cortical network dysfunction caused by a subtle defect of myelination. *Glia*, *64*(11), 2025–2040. <https://doi.org/10.1002/glia.23039>
- Purves, D., Augustine, G. J., Fitzpatrick, D., Katz, L. C., LaMantia, A.-S., McNamara, J. O., & Williams, S. M. (Eds.). (2001). Increased Conduction Velocity as a Result of Myelination. In *Neuroscience* (2nd ed.). Sunderland: Sinauer Associates.
- Qiu, L. R., Fernandes, D. J., Szulc-Lerch, K. U., Dazai, J., Nieman, B. J., Turnbull, D. H., ... Lerch, J. P. (2018). Mouse MRI shows brain areas relatively larger in males emerge before those larger in females. *Nature Communications*, *9*(1). <https://doi.org/10.1038/s41467-018-04921-2>
- Quarles, R. H., Macklin, W. B., & Morell, P. (2006). Myelin Formation, Structure, and Biochemistry. In G. J. Siegel (Ed.), *Basic Neurochemistry: Molecular, Cellular, and Medical Aspects* (pp. 51–71). Elsevier. Retrieved from <https://pdfs.semanticscholar.org/9ab6/d7a3ac38c5efae623030ca7fb9bf4104069a.pdf>
- Regenold, W. T., Phatak, P., Marano, C. M., Gearhart, L., Viens, C. H., & Hisley, K. C. (2007). Myelin staining of deep white matter in the dorsolateral prefrontal cortex in schizophrenia, bipolar disorder, and unipolar major depression. *Psychiatry Research*, *151*(3), 179–188. <https://doi.org/10.1016/j.psychres.2006.12.019>
- Richards, K., Watson, C., Buckley, R. F., Kurniawan, N. D., Yang, Z., Keller, M. D., ... Reutens, D. C. (2011). Segmentation of the mouse hippocampal formation in magnetic resonance images. <https://doi.org/10.1016/j.neuroimage.2011.06.025>
- Richardson, W. D., Emery, B., Ohayon, D., Li, H., Paes de Faria, J., Tohyama, K., & McKenzie, I. A. (2014). Motor skill learning requires active central myelination. *Science*, *346*(6207), 318–322. <https://doi.org/10.1126/science.1254960>
- Rodgers, R. J., & Cole, J. C. (1993). Influence of social isolation, gender, strain, and prior novelty on plus-maze behaviour in mice. *Physiology and Behavior*, *54*(4), 729–736. [https://doi.org/10.1016/0031-9384\(93\)90084-S](https://doi.org/10.1016/0031-9384(93)90084-S)
- Scherer, S. S. (1997, January 1). Molecular genetics of demyelination: New wrinkles on an old

- membrane. *Neuron*. Elsevier. [https://doi.org/10.1016/S0896-6273\(01\)80042-8](https://doi.org/10.1016/S0896-6273(01)80042-8)
- Scholz, J., Klein, M. C., Behrens, T. E. J., & Johansen-Berg, H. (2009). Training induces changes in white-matter architecture. *Nature Neuroscience*, *12*(11), 1370–1371. <https://doi.org/10.1038/nn.2412>
- Schubert, M. I., Porkess, M. V., Dashdorj, N., Fone, K. C. F., & Auer, D. P. (2009). Effects of social isolation rearing on the limbic brain: A combined behavioral and magnetic resonance imaging volumetry study in rats. *Neuroscience*, *159*(1), 21–30. <https://doi.org/10.1016/j.neuroscience.2008.12.019>
- Schultze, M., & Rudneff, M. (1865). Weitere Mittheilungen über die Einwirkung der Ueberosmiumsäure auf thierische Gewebe. *Archiv Für Mikroskopische Anatomie*, *1*(1), 300–304. <https://doi.org/10.1007/BF02961418>
- Schwann, T. (1911). Mikroskopische Untersuchungen über die Übereinstimmung in der Struktur und dem Wachstume der Tiere und Pflanzen. *Nature*, *86*(2158), 41–41. <https://doi.org/10.1038/086041a0>
- Steadman, P. E., Ellegood, J., Szulc, K. U., Turnbull, D. H., Joyner, A. L., Henkelman, R. M., & Lerch, J. P. (2014). Genetic Effects on Cerebellar Structure Across Mouse Models of Autism Using a Magnetic Resonance Imaging Atlas. *Autism Res*, *7*, 124–137. <https://doi.org/10.1002/aur.1344>
- Taveggia, C., Feltri, M. L., & Wrabetz, L. (2010). Signals to promote myelin formation and repair. *Nature Reviews Neurology*. <https://doi.org/10.1038/nrneurol.2010.37>
- Tomlinson, L., Leiton, C. V., & Colognato, H. (2016, November 1). Behavioral experiences as drivers of oligodendrocyte lineage dynamics and myelin plasticity. *Neuropharmacology*. Pergamon. <https://doi.org/10.1016/j.neuropharm.2015.09.016>
- Toua, C., Brand, L., Möller, M., Emsley, R. A., & Harvey, B. H. (2010). The effects of sub-chronic clozapine and haloperidol administration on isolation rearing induced changes in frontal cortical N-methyl-d-aspartate and D1 receptor binding in rats. *Neuroscience*, *165*(2), 492–499. <https://doi.org/10.1016/j.neuroscience.2009.10.039>
- Ullmann, J. F. P., Watson, C., Janke, A. L., Kurniawan, N. D., & Reutens, D. C. (1975). Meltzer and Ryugo, 2006) and gene expression studies.

- <https://doi.org/10.1016/j.neuroimage.2013.04.008>
- Valzelli, L. (1973). The “isolation syndrome” in mice. *Psychopharmacologia*, *31*(4), 305–320.
<https://doi.org/10.1007/BF00421275>
- van Eede, M. C., Scholz, J., Chakravarty, M. M., Henkelman, R. M., & Lerch, J. P. (2013). Mapping registration sensitivity in MR mouse brain images. *NeuroImage*, *82*, 226–236.
<https://doi.org/10.1016/j.neuroimage.2013.06.004>
- Venkatesan, R., Lin, W., & Haacke, E. M. (1998). Accurate determination of spin-density and T1 in the presence of RF- field inhomogeneities and flip-angle miscalibration. *Magnetic Resonance in Medicine*, *40*(4), 592–602. <https://doi.org/10.1002/mrm.1910400412>
- Vesalius, A. (1543). *Andrae Vesalii Bruxellensis, scholae medicorum Patavinae professoris, de Humani corporis fabrica Libri septem*. Basileae: [ex officina Ioannis Oporini].
<https://doi.org/10.3931/e-rara-20094>
- Voss, M. W., Heo, S., Prakash, R. S., Erickson, K. I., Alves, H., Chaddock, L., ... Kramer, A. F. (2013). The influence of aerobic fitness on cerebral white matter integrity and cognitive function in older adults: Results of a one-year exercise intervention. *Human Brain Mapping*, *34*(11), 2972–2985. <https://doi.org/10.1002/hbm.22119>
- Wang, C., Wu, C., Popescu, D. C., Zhu, J., Macklin, W. B., Miller, R. H., & Wang, Y. (2011). Longitudinal near-infrared imaging of myelination. *Journal of Neuroscience*, *31*(7), 2382–2390. <https://doi.org/10.1523/JNEUROSCI.2698-10.2011>
- Weiss, I. C., Pryce, C. R., Jongen-Rêlo, A. L., Nanz-Bahr, N. I., & Feldon, J. (2004). Effect of social isolation on stress-related behavioural and neuroendocrine state in the rat. *Behavioural Brain Research*, *152*(2), 279–295. <https://doi.org/10.1016/j.bbr.2003.10.015>
- Wongwitdecha, N., & Marsden, C. A. (1996). Effects of social isolation rearing on learning in the Morris water maze. *Brain Research*, *715*(1–2), 119–124. [https://doi.org/10.1016/0006-8993\(95\)01578-7](https://doi.org/10.1016/0006-8993(95)01578-7)
- Yamamuro, K., Yoshino, H., Ogawa, Y., Makinodan, M., Toritsuka, M., Yamashita, M., ... Kishimoto, T. (2018). Social Isolation During the Critical Period Reduces Synaptic and Intrinsic Excitability of a Subtype of Pyramidal Cell in Mouse Prefrontal Cortex. *Cerebral Cortex (New York, N.Y. : 1991)*, *28*(3), 998–1010. <https://doi.org/10.1093/cercor/bhx010>

Zhao, Y.-Y., Shi, X.-Y., Qiu, X., Lu, W., Yang, S., Li, C., ... Tang, Y. (2012). Enriched Environment Increases the Myelinated Nerve Fibers of Aged Rat Corpus Callosum. *The Anatomical Record: Advances in Integrative Anatomy and Evolutionary Biology*, 295(6), 999–1005. <https://doi.org/10.1002/ar.22446>